



Experimental Study and Quantum Calculations for Spiramycin and Isosorbide Dinitrate as Corrosion Inhibitors

¹Thekra Abd Alkarim, ¹Khalida F. Al-Azawi*, ²Rana Afif Anaee

¹Applied Chemistry Branch, Department of Applied Sciences, University of Technology – Iraq

²Department of Materials Engineering, University of Technology – Iraq

Article information

Article history:

Received: March, 02, 2022

Accepted: May, 19, 2022

Available online: March, 10, 2023

Keywords:

Expired Drugs,
Corrosion inhibition,
Aluminum,
Tafel plot

*Corresponding Author:

Khalida F. Al-Azawi
100122@uotechnology.edu.iq

Abstract

The investigation of the efficiency of two expired drugs, including Spiramycin and Isosorbide dinitrate, was done as corrosion inhibitors for aluminum in 0.1M HCl medium using the electrochemical method by Potentiostat at four temperatures (293, 303, 313, and 323 K) and 200 ppm as constant concentration for each drug. The results showed that these drugs gave good efficiencies equal to 98.836% and 94.285 % for Spiramycin and Isosorbide dinitrate at 293 K, respectively, by adsorption process on the metallic surface. They act as mixed-type inhibitors due to shifting corrosion potential either to active or noble direction. The corrosion data were measured and debated, where the corrosion current density was decreased after adding expired drugs to the corrosive medium due to inhibiting the cathodic and anodic reactions (i.e., the dissolution and reduction reactions). Using SEM exam, the inhibited surface of specimens was characterized to confirm the coverage of the surface by drug molecules. The adsorbed layer by Spiramycin was better than that by Isosorbide dinitrate. Also, the Fourier transform infrared spectra were used to limit the active site attracted to the surface by adsorption that confirmed the attraction by hydroxyl and nitro groups, as illustrated by the mechanism of inhibition. In addition, the antibacterial activity of the inhibitors against some types of bacteria was tested to confirm the formation of an inhibition zone against bacteria. The quantum chemical parameters exhibited a good correlation with the inhibition efficiency.

DOI: [10.53293/jasn.2022.4763.1143](https://doi.org/10.53293/jasn.2022.4763.1143), Department of Applied Science, University of Technology
This is an open access article under the CC BY 4.0 license.

1. Introduction

Corrosion is the deterioration of metal by chemical attack or reaction with its environment [1] Considered an economic problem for most industrialized countries. It affects all sectors of production and transportation. One of the most practical ways to protect against the dissolution of metals by corrosion is the use of appropriate inhibitors [2]. Organic corrosion inhibitors are important for corrosion control and mitigation. Compounds containing bonds, phenyl rings, conjugated double bonds, heteroatoms (N, S, O, P), and other heteroatoms are the most effective and efficient organic inhibitors. A significant majority of these chemical molecules, e.g.,

pyridines, furans, imidazoles, thiophenes, isoxazoles, etc., have a lot in common with the substructures of a lot of regularly used medicines. This property has motivated researchers worldwide to investigate the use of medicines as corrosion inhibitors. These inhibitors slow down corrosion via (i) adsorption of ions/molecules onto the metal surface, and (ii) increasing or reducing the anodic and/or cathodic reaction. (iii) decreasing the diffusion rate of reactants to the metal surface, (iv) decreasing the electrical resistance of the metal surface, and (v) inhibitors that are frequently easier to apply and have an advantage in situ application. When selecting an inhibitor, several factors need to be considered, including cost and quantity, ease of availability, and, most importantly, safety to the ecosystem and its species. Some of the most potent inorganic inhibitors are carbonates, nitrites, chromates, silicates, and phosphates. Still, chromates and zinc salts are being phased out and are being substantially replaced with organic inhibitors because of their toxicity. Many of the commonly used drugs' substructures are strikingly similar. This characteristic has prompted researchers worldwide to investigate the use of drugs as corrosion inhibitors. In addition to being promising corrosion inhibitors, it was discovered that the expired drugs [3]. Many researchers highlighted using expired drugs, considered green and eco- friendly inhibitors to protect aluminum in different applications [4–17]. They have proven to be good inhibitors; these studies used polarization measurements of the inhibition process as well as thermodynamic, kinetic studies and adsorption isotherms [18–26]. The present work aims to study of two expired drugs as corrosion inhibitors with a concentration of 200 ppm at four temperatures (293,303, 313 and 323 K) for aluminum in HCl environment in addition to test the antibacterial activity of these inhibitors.

2. Materials and Methods

2.1. Chemicals

Squire-shaped samples were cut off from pure aluminum (2×2 cm) using cutting tool (Wire Cut) in the University of Technology / Training, and had the chemical composition mentioned below: Si (0.41), Fe (0.40), Cu (0.11), Mn (0.040), Mg (0.04), Cr (0.0), Zn (0.10), Ti (0.0) and Al (99.0 %). After that, the samples were ground and polished with emery papers (600 to 3000) with alumina suspension ($1\mu\text{m}$) to achieve a smooth surface. After that, the polished samples were degreased with ethanol, washed with distilled water, then dried, and put in plastic containers to be ready for electrochemical experiments. The 0.1 M HCl test solution was made by diluting an analytical grade stock (Merck) with water. Drugs were bought from pharmacy and extracted in the laboratory. 200ppm spiramycin was dissolved in ethanol, while 200 isosorbide dinitrate was dissolved in water and then added to the corrosive medium. The chemical structure of these drugs is shown in Figures 1 and 2.

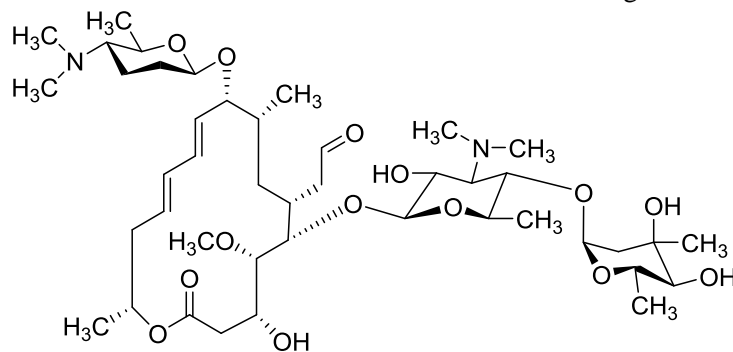


Figure 1: Chemical structure of Spiramycin structure.

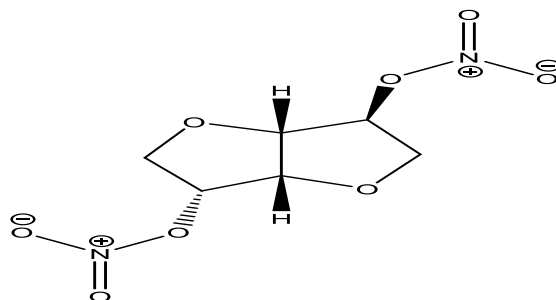


Figure 2: Chemical structure of Isosorbide dinitrate structure.

2.2. Polarization Experiments

potentiostat / galvanostat (WINKINK M Lab 200) was utilized for polarization test in this study with system of three electrodes: pure platinum (auxiliary), saturated calomel (reference electrode) and pure aluminum (working electrode). 0.1 HCl solution was prepared, and the specimens were immersed in corrosive solution (with or without inhibitor). All experiments were performed at 20, 30, 40 and 50 °C using a water bath to control the temperature. The Tafel extrapolation method was used to measure the corrosion potential (E_{corr}), corrosion current density (i_{corr}), and Tafel slopes (β_c and β_a).

2.3. Surface Inspections

Aluminum specimens were tested before and after corrosion (absence and presence of inhibitors) by SEM. the topography of the surface is measuring using energetic electron beams because the shorter wavelength of electrons allows image magnifications higher than conventional light microscopy where react electrons with atoms to make signals that contain information about the samples surface topography. FT-IR analyses are useful for discussing the activity of inhibitors and characterization of the chemical for drugs was selected in powder and film. Fourier transform infrared of the films formed on the aluminum surface was recorded by FT-IR-8400 Shimadzu.

2.4. Biological Activity

In this work, antimicrobial efficiency was studied by well diffusion method to explain the activity of microbial of the inhibitors on some gram (+Ve) and gram (-Ve) bacteria as *Staphylococcus aureus*, *Streptococcus epidermidis*, and *Escherichia coli* and *Klebsiella sp*(-Ve) and *Candida albicans*. Suspension from the main culture was isolated with 4 mL of normal saline into a test tube. It was distributed on agar medium (Mueller Hinton) and was left for 10 min to dry. Four wells (8 mm) were cut from the agar by a sterile cork-borer, and 50 μ L of concentration of the inhibitor (200 ppm) was added to the wells. The Petri plates were incubated for 24 h at 310 K to grow the bacteria. The diameter of the zone of inhibition was measured (in mm) and used as a measure of antimicrobial activity.

3. Results and Discussion

3.1. Potentiodynamic Measurements

Polarization curves of aluminum specimens in HCl solution at the selected temperatures (293,303, 313 and 323 K) were shown in Figure 3, which show the generated Al^{3+} at the anodic site and evolution H^+ at the cathodic site. While Tafel polarization curves in the presence 200 ppm of two drugs (Spiramycin and Isosorbide dinitrate) at the selected temperatures were illustrated in Figure 4 a and b. The polarization results of aluminum specimens in HCl solution with and without of the two drugs were elucidated in Table 1, where the values of E_{corr} are shifted to either more positive or more negative value that indicated these compounds behaved as a mixed-type inhibitor, i.e., these compounds inhibit or delay the reactions occurring at the cathode (reduction of hydrogen) and prevent further oxidation (dissolution of the aluminum) at anode through a formation of the adsorbed layer on the aluminum surface by attraction process for functionally groups or any electronic density in drug molecules to positively charged Al surface. Also, this behavior is confirmed through the decrease in the Tafel slopes of the cathodic and anodic regions (β_c and β_a , respectively) which indicates the lower change in current corresponding to applied potential after coverage by drug clustering. From Table 1, it was noted that the values of i_{corr} and C_R values have decreased and C_R values were calculated from Eq. (1) [27]:

$$C_R mpy = 0.13 \times i_{corr} \times \left(\frac{e}{\rho}\right) \quad (1)$$

Where C_R : rate of corrosion, e : aluminum equivalent weight and ρ : aluminum density. The coverage areas by the inhibitor can occur through the formation of the Al^{3+} —drug complex. At different temperatures, it can be seen that the corrosion potential was varied because of variation in reaction sites at the anodic and cathodic areas after coverage. While the corrosion current density was increased with increasing temperature due to increasing the energy of particles and increasing the rate of transferring mass and charge leading to an increase in the rate of reactions. The values of IE% were calculated according to Eq. (2) [28_29]:

$$IE\% = \left[1 - \frac{i_{\text{corr, inhibited}}}{i_{\text{corr, uninhibited}}} \right] \times 100 \quad (2)$$

Where IE%: the inhibition efficiency, i_{corr} (inhibited) and i_{corr} (uninhibited) are the corrosion current density with and without inhibitor, respectively. The added compounds inhibit the corrosion process by adsorption on aluminum surface to form a barrier between the metallic surface and corrosive environment. The values of IE% show that the two drugs are good inhibitors; at a constant temperature, Spiramycin gives efficiency better than Isosorbide dinitrate. These inhibitor molecules work through an adsorption mechanism by the functional groups in the chemical structure, such as —OH and —NO₂ groups in their chemical structures in addition to N and O heteroatoms within the heterocyclic rings that were attracted to the charged metal surface.

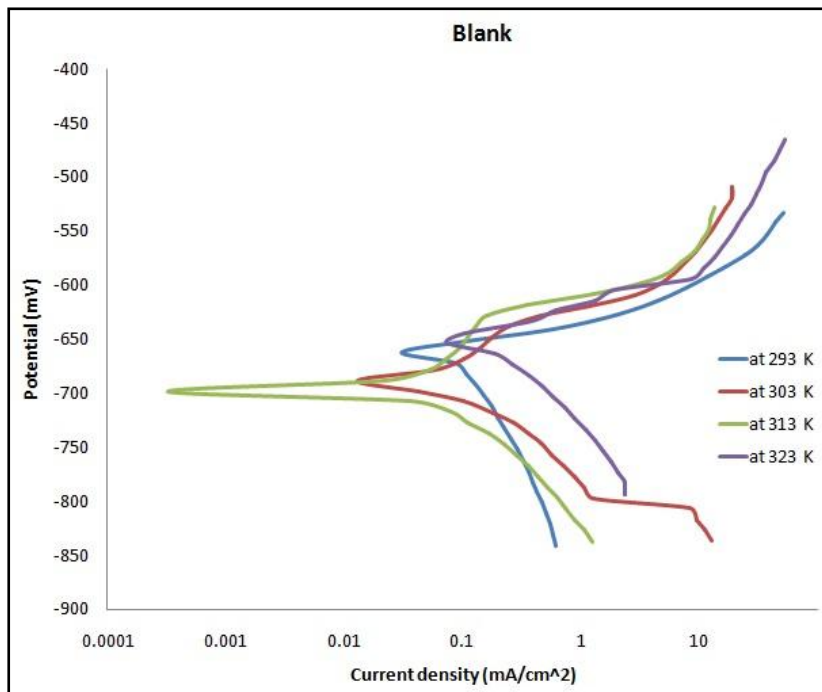
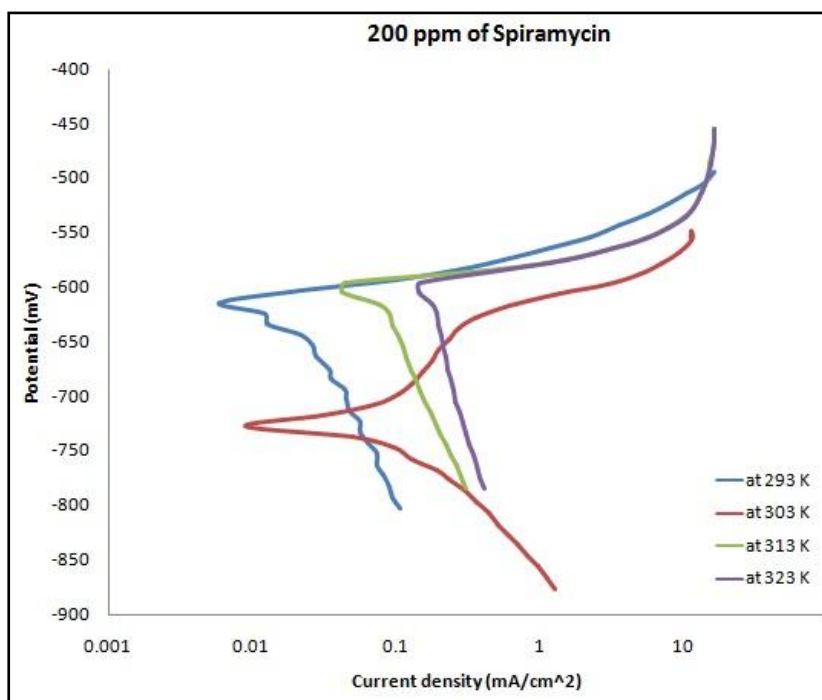


Figure 3: Tafel plot of aluminum in HCl at four temperatures.



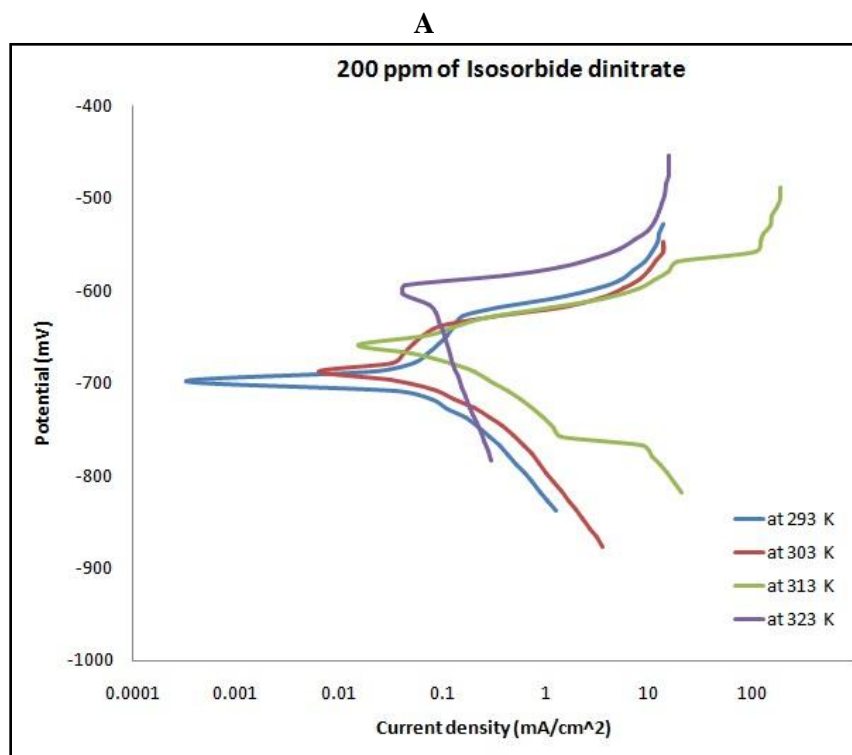


Figure 4: Tafel plot of aluminum in HCl in the presence of (A) Spiramycin and (B) Isosorbide dinitrate at four temperatures.

Table 1: Corrosion data for polarization of inhibition in HCl medium in the absence and presence of 200 ppm of two inhibitors at four temperatures.

Inhibitor	Temp. (K)	-E _{corr} (mV)	i _{corr} (μA.cm ⁻²)	-b _c	+b _a	C _R (mpy)	IE (%)
				(mV.dec ⁻¹)			
Blank	293	664	147	195.4	69.2	63.693	---
	303	688	213	90.0	254.8	92.290	---
	313	751	240	119.3	88.8	103.989	---
	323	656.5	393.4	58	162.6	170.456	---
Spiramycin	293	698	1.71	12.6	32.6	0.740	98.836
	303	687	7.37	54.9	28.3	3.193	96.539
	313	659	9.5	23.9	36.5	4.116	96.041
	323	663.1	43.34	39.6	29.6	18.778	88.983
Isosorbide dinitrate	293	613	8.4	87.1	20.9	3.639	94.285
	303	725.8	12.09	26.6	28.3	5.238	94.323
	313	725	20.46	28.3	41.6	8.865	91.475
	323	671.7	69.15	17.2	59.4	29.962	82.422

3.2. SEM Analyses

The morphology images in Figure 5 shows that the polished metal's surface was smooth. In contrast, in Figure 6, the corroded samples appear significant surface damage in both the anode and cathode regions in addition to some cracks, corrosion products and damaged passive layer of Al_2O_3 by the acidic medium. The inhibitor covered the surface of inhibited samples as clusters of drug molecules to isolate the Al surface from acidic attack

and getting smoother surface as shown in Figure 7, also can be seen that the coverage by Spiramycin is better than Isosorbide dinitrate.

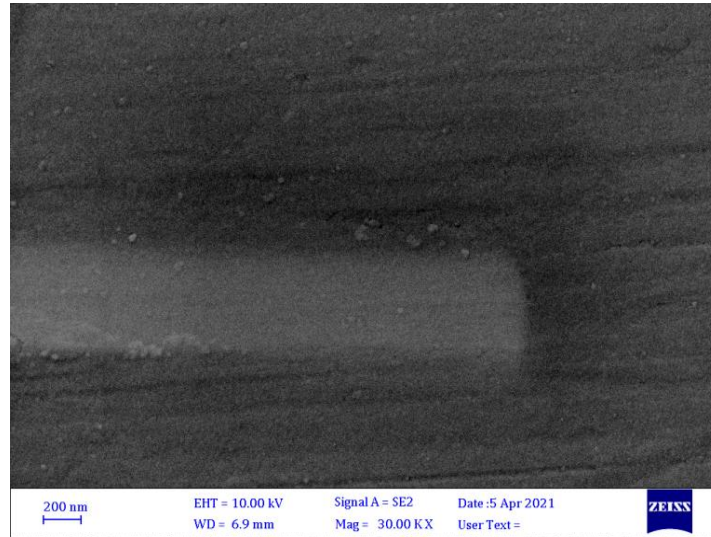


Figure 5: SEM images for the polished surface.

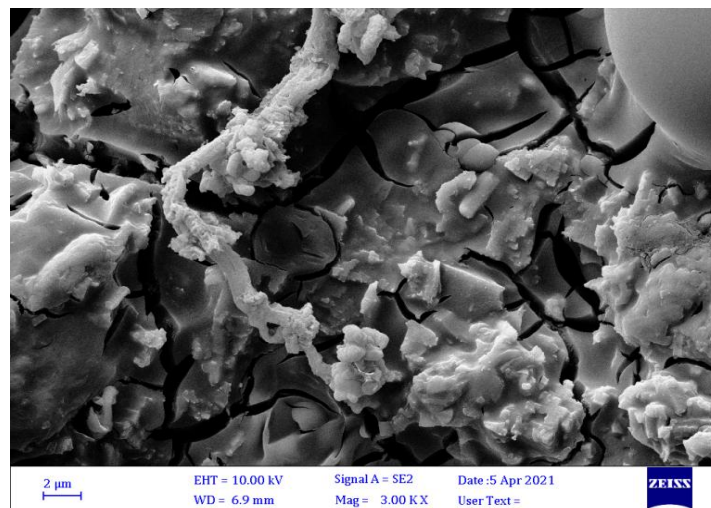
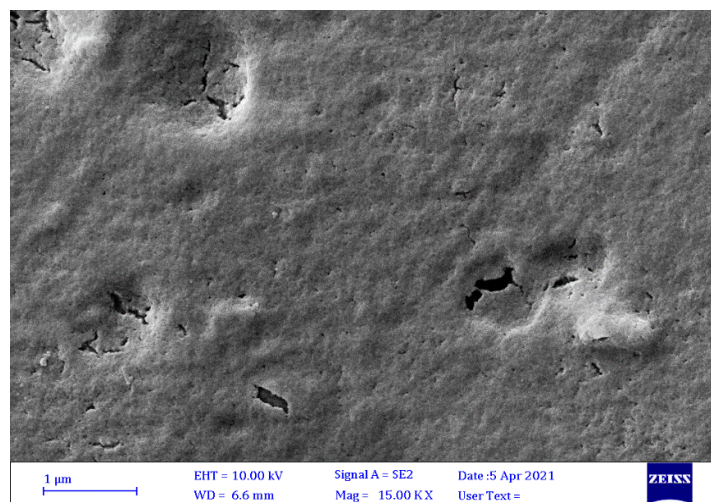


Figure 6: SEM images after corrosion in HCl medium.



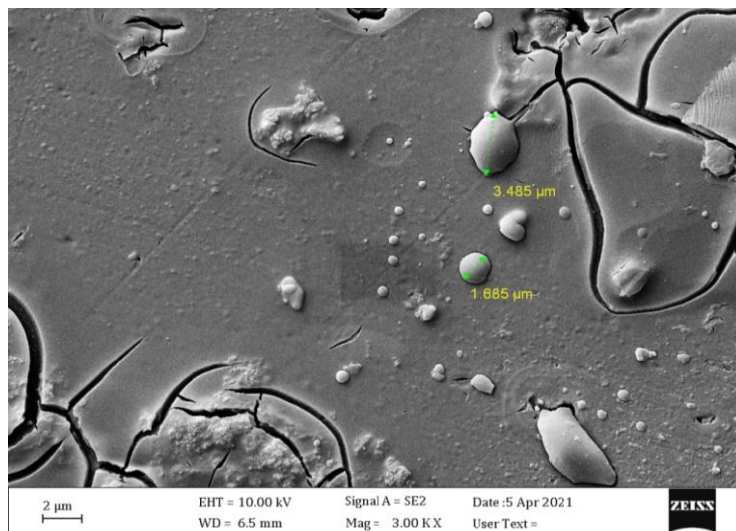


Figure 7: SEM images after inhibition with two inhibitors in HCl medium.

3.3. FTIR

The FT-IR spectroscopy technique has been utilized to identify the differences between the stretching and vibration of the functional groups in Spiramycin inhibitor and a scratch layer Spiramycin adsorbed on the surface of aluminum. Figure 8 illustrates the FT-IR spectra of Spiramycin inhibitor and the adsorbed film on the metal surface: the peak at 3485 cm^{-1} is attributed to O-H stretching vibration, for stretching of C-H aliphatic at 2933 cm^{-1} in addition to that C=O stretching appear at 1722 cm^{-1} and C=C stretching aromatic is around 1675 cm^{-1} . C-N and C-O exhibited in the range from 1000 to 1350 cm^{-1} . FTIR spectrum for the extracted Isosorbide dinitrate is illustrated in Figure 9.

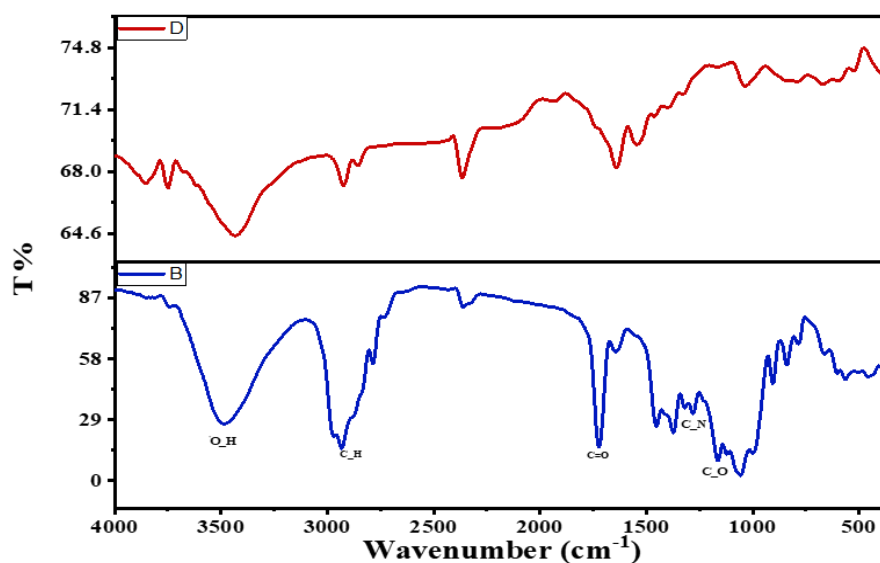


Figure 8: FTIR spectra of Spiramycin (blue line) and film formed after adsorption on aluminum surface (red line 200 ppm).

The presence of an O-H group leads to three modes of vibration, viz. stretching, inplane bending and out of the plane bending vibrations. Wide bands in the range $3600\text{--}3400\text{ cm}^{-1}$ describe O-H stretching vibrations. These vibrations are more delicate towards hydrogen bonding. The frequency of stretching and bending vibrations changes when a hydrogen bond is present. In hydrogen bonded species, these bands shift to a lower frequency of

greater amplitude, and the band broadens. The O–H stretching band will be reduced to $3550\text{--}3200\text{ cm}^{-1}$ in the presence of hydrogen bonding in a five or six member ring structure [30]. The peak at 2899 cm^{-1} is attributed to C–H aliphatic stretching. The asymmetric NO_2 stretching vibrations are found in the region 1654 cm^{-1} , whereas the symmetric NO_2 stretching vibrations are expected to be in the region 1386 cm^{-1} . The intensity of all stretching bands measured in Spiramycin and isosorbide dinitrate was clearly reduced in the FT-IR spectra of the inhibited layer. The functional groups and active centers in inhibitors interacted with the Al surface and produced a protective coating against corrosion, especially for the —OH group, as shown by the results. This indicates that this group is attracted to the metal by adsorption to form Al-drug complex.

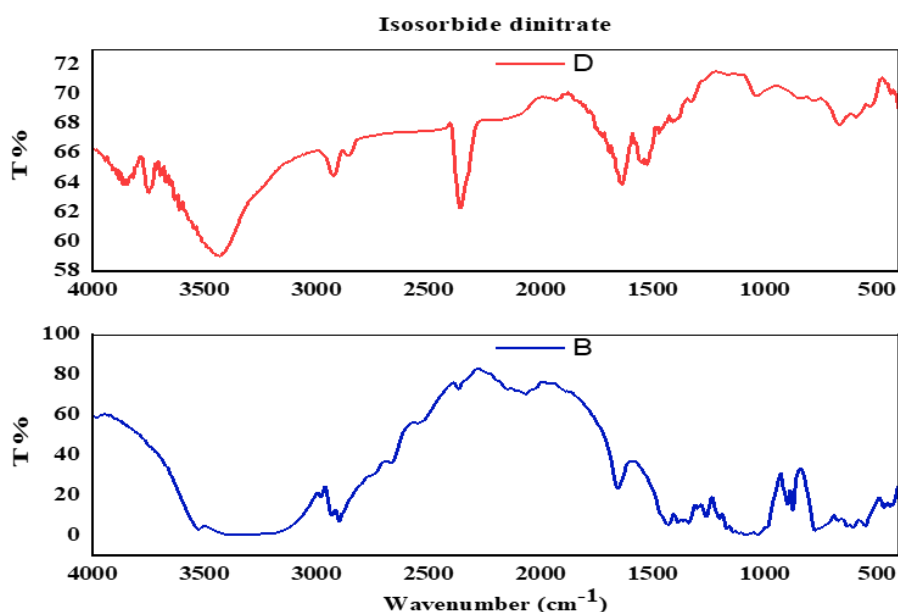


Figure 9: FTIR spectrum for Isosorbide dinitrate (blue line) and after adsorption on an aluminum surface, a film is formed (red line 200 ppm).

3.4. Antimicrobial Test of the Inhibitors

The antimicrobial activity of the expired drugs was investigated using the well diffusion method to show the zone of inhibition activity in 200 ppm of each compound. The antimicrobial properties of the expired drugs induced cell death. Spiramycin and Isosorbide dinitrate has a good antibacterial activity against both gram positive and negative bacterial cultures. The inhibition zone against bacteria was measured in mm and the related results are listed in Table 2.

Table 2: Data of antimicrobial test for 200 ppm of inhibitors.

Type of bacteria	Spiramycin	Isosorbide dinitrate
<i>Staphylococcus aureus</i>	43	25
<i>Staphylococcus epidermidis</i>	45	25
<i>Escherichia coli</i>	26	25
<i>Klebsiella sp.</i>	25	25
<i>Candida albicans</i>	45	30

3.5. Inhibition Mechanism

The expired drugs act as corrosion inhibitors for aluminum in 0.1 M HCl by adsorbing on anodic sites due to the hetero atoms in drug structure (N and O atoms). In addition, the molecules contain high electron densities that strongly interact with the positive charge of Al ions at pure aluminum /solution interface, forming Al ion/drug complexes. These complexes act as a barrier to shield the metallic surface from the corrosive medium. This adsorption is achieved through functionally groups that have an electronic density as pairs of free electron or π

electrons that interact by nucleophile attacks and facilitate the adsorption process on the surface of the metal. In the present compounds, it can be seen hydroxyl and nitrate groups in addition to electron pairs on O and N atoms. Figure 10 shows the mechanism of inhibition after adsorption two drugs on aluminum surface by attracting different charges.

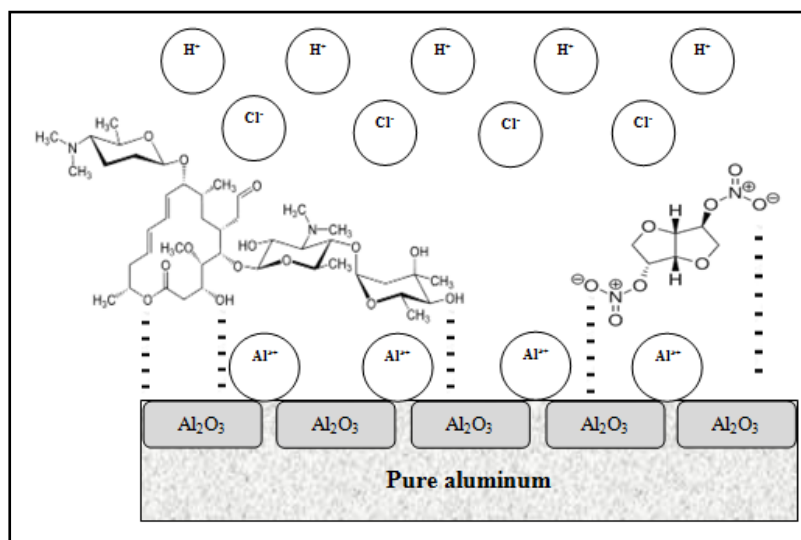


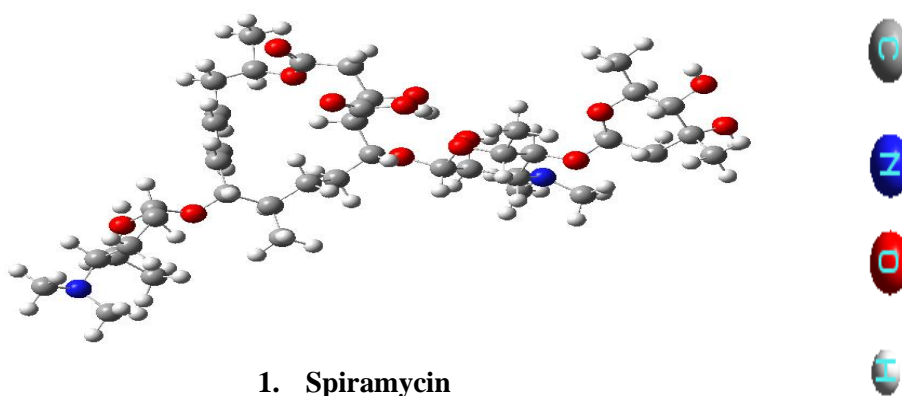
Figure 10: Mechanism of corrosion inhibition by drugs.

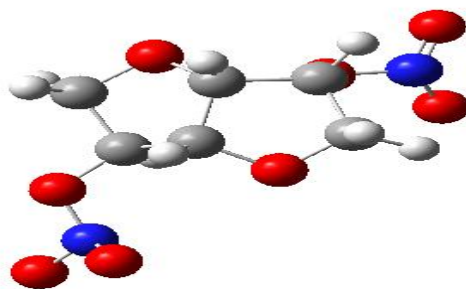
4. Quantum Calculations

Quantum calculation use in inhibition field to prediction of the activity of selected inhibitors [31–33]. The 6-311G (d,p) base set and Density Functional Theory (DFT) were used. Physical properties such as (ionization energy, dipole moment, hardness, and softness) of (Spiramycin and Isosorbide dinitrate) compounds were calculated using occupied orbitals, energy gap, and physical properties such as (ionization energy, dipole moment, hardness, and softness). In addition, the total electron density (TED) and the Electrostatic Surface Potential (ESP) functions are discussed.

4.1. Theoretical Part

Two software programs were used during the present work. The quantum chemical calculations were carried out using Gaussian 09 software and density functional theory (DFT) with a hybrid function of Becke three-parameters Lee, Yang, and Parr (B3LYP). The 6-311G (d,p) basis set was chosen because it provides accurate electronic properties and geometries for a wide range of organic compounds Figure 11, while also producing comparable results. The calculations have been conducted in the vacuum medium [34–36].





2. Isosorbide dinitrate

Figure 11: Equilibrium geometry of the inhibitors molecules calculated by DFT (B3LYP/6-311G (d,p)) method.

4.2. Inhibitors Parameters

The prediction of adsorbed inhibitor molecules was done by limits orbital theory respected to centers of these molecules to be attracted to the metal surface [37]. The molecular orbital boundary (FMO), which contributes to the authoritarian contribution via the inverse of the energy dependency of the stability of the difference in orbital energy as $E = E_{\text{LUMO}} - E_{\text{HOMO}}$, contributes to the authoritarian contribution. The energy HOMO (E_{HOMO}) is a measure of a molecule's propensity to transfer an electron to an acceptor, and the molecule inhibitor has a high E_{HOMO} value, indicating that it has a tendency to donate electrons. The LUMO energy (E_{LUMO}) is the ability of a molecule to absorb an electron, and the lower the value, the larger the electron-accepting potential, from Table 3 can be seen that Spiramycin has higher (E_{HOMO}) than Isosorbide dinitrate, i.e., Spiramycin adsorb on the surface better than other drug and this result agreement with experimental data. Another important factor in describing molecular activity is the energy gap between orbital borders (E); as the energy gap narrows, the inhibitor's performance improves [38]. Chemical quantum parameters such as the highest occupied molecular orbital by electrons (E_{HOMO}), the energy of the lowest unoccupied molecular orbital (E_{LUMO}), and the energy of the lowest unoccupied molecular orbital (E_{LUMO}) are shown in Tables 3 and 4. (E_{LUMO}), The energy gap ($E = E_{\text{LUMO}} - E_{\text{HOMO}}$), dipole moment (μ), electronegativity (EP), ionization potential (IP), electron affinity (EA), and global softness (S) were all found to be related to molecule inhibition efficiency. The ionization potential (IP) and electronic affinity (EA) were related to the negative HOMO energy and LUMO energy, respectively, according to Koopman's [39] theory:

$$IP = -E_{\text{HOMO}} \quad (3)$$

IP is the amount of energy available to remove an atom's electron. Because of the low ionization energy, inhibition is highly effective.

$$EA = -E_{\text{LUMO}} \quad (4)$$

EA is the amount of energy emitted when an electron is applied to a neutral atom. The greater the value of electron affinity, the less stable the system is and the more effective inhibition must be. Hardness (η) has been defined as the second derivative of the E that measures both the stability and reactivity of the molecule [40].

$$\eta = \frac{IP - EA}{2} \quad (5)$$

$$X = -\mu = \frac{IP + EA}{2} \quad (6)$$

The HOMO and LUMO energies were associated with these values. A low electronegativity value indicates a high inhibition efficiency. Global softness (S) is the inverse of global hardness (H) [39]. Softness is an important property for determining molecular stability and reactivity:

$$S = \frac{1}{\eta} \quad (7)$$

The global electrophilicity index (ω) was developed by Parr [41] and is a calculation of energy stability after a molecule accepts an additional sum of electrons. A lower global electrophilicity index value denoted a strong inhibitor.

$$\omega = \frac{(-X)^2}{2\eta} \quad (8)$$

The order of inhibition values according to quantum parameters took the following sequences; HOMO was $2 > 1$, LUMO was $1 > 2$, ΔE was $1 > 2$, μ was $1 > 2$, IE was $1 > 2$, EA was $2 > 1$, χ was $1 > 2$, η was $1 > 2$, S was $1 > 2$, and ω was $1 > 2$. While the final order of the inhibitors efficiency was $1 > 2$.

Table 3: DFT was used to calculate the physical parameters of the inhibitor molecule in a vacuum medium at ground state equilibrium geometries.

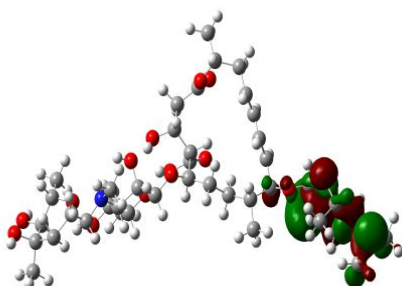
Comp.	E _{HOMO} (eV)	E _{LUMO} (eV)	$\Delta E_{\text{HOMO-LUMO}}$ (eV)	μ (Debye)
<i>Spiramycin</i>	-5.07422164	-1.7263293	3.347892	7.952
<i>Isosorbide dinitrate</i>	-7.75297092	-3.9171674	3.835804	5.802

Table 4: The DFT approach was used to derive quantum chemical properties for the inhibitor molecule in a vacuum medium.

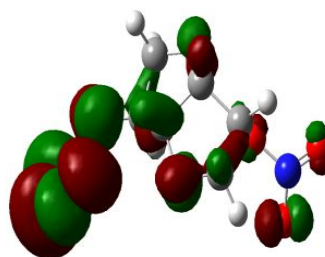
Inhib.	IE (eV)	EA (eV)	χ (eV)	η (eV)	S (eV)	ω (eV)
<i>Spiramycin</i>	5.07422	1.7263	3.40027	1.67394	0.59739	3.45347
<i>Isosorbide dinitrate</i>	7.75297	3.9171	5.83506	1.91790	0.52140	8.87637

Figure 12 illustrates the optimization of geometries of molecules analyzed in the gas phase, including LUMO and HOMO density distributions. The red color represents high electron density, while the green color represents low electron density [42]. High electron density is a donating area of electrons to the metal surface. The Green area is the reception of electrons from the metal surface [43]. Therefore, the distribution of these two areas is very important. Inhibitor number 1 had a high electron density from the receptor site, and the double bond is the reason in O atom with the nonbonding electrons ring. While inhibitor 2 seems to the receptors on N atom and donate by N with (NO₃) groups.

Spiramycin



2. Isosorbide dinitrate



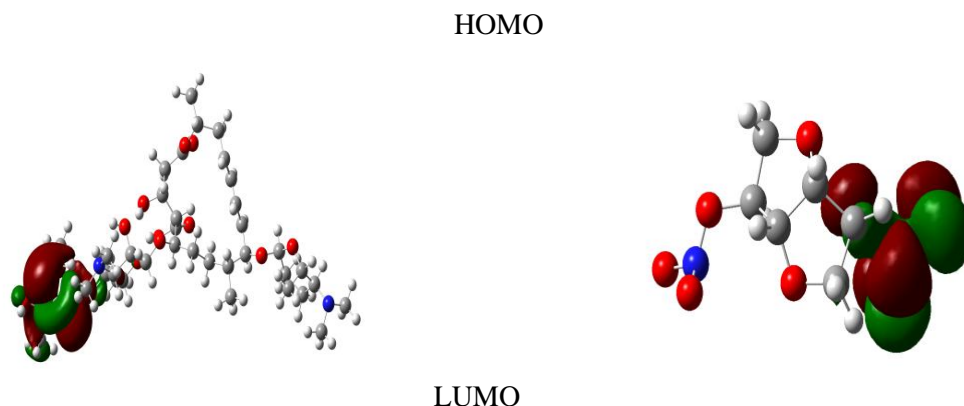
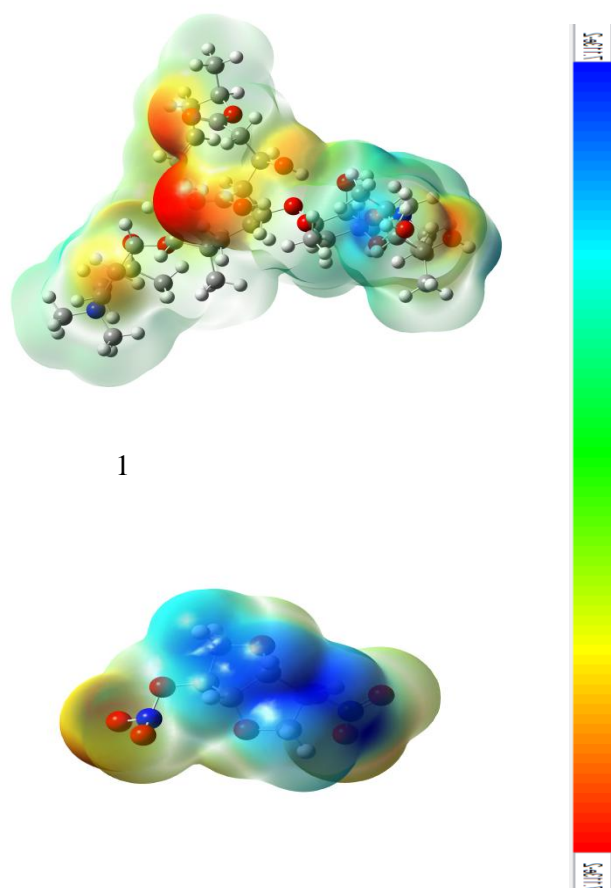


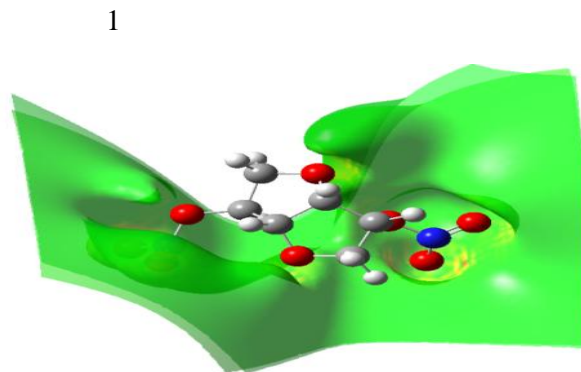
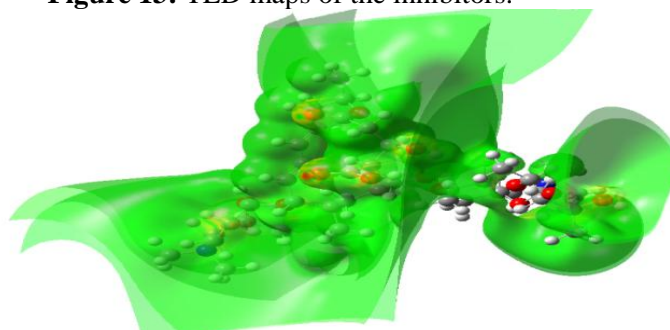
Figure 12: The energy levels (HOMO-LUMO) orbitals of the studied inhibitors (1 and 2).

4.3. Electron Density Maps

The strength of the adsorption link is determined by the electron density of the donor atom. The density of electrons on the molecule was represented by total electron density (TED). The red color suggests high electron negativity regions in investigated molecules, such as the (O) atom and certain parts of the (NH₂), which can aid in the electrophilic attack, as seen in Figure 13. These atoms have a moderate electronegativity in addition to their yellow color. The highest positive area capable of receiving electrons from the donor chemical is indicated by the blue area. [43]. The direct contacts of compounds 1 and 2 with the metal surface are known as electrostatic surface potential (ESP). Parts of the compounds containing atoms with a high electron density and planarity are not active at the moment Figure 14.



2
Figure 13: TED maps of the inhibitors.



2
Figure 14: ESP map of the studied compounds.

5. Conclusions

Expired drugs (Spiramycin, Isosorbide dinitrate) with concentration (200 ppm) were good inhibitors to protect pure aluminum in 0.1M of HCl solution at (293,303,213 and 323K) and they classified as a mixed-type inhibitor with an inhibition efficiency reached to 98.84 % at 293 K for Spiramycin and to 94.3% at 303 K for isosorbide dinitrate. In addition to the biological activity of Spiramycin and isosorbide dinitrate against corrosive bacteria which indicates the good antimicrobial activity against both gram positive and negative bacterial cultures. All results were supported by SEM and FT-IR tests. Quantum calculations limit the amount of active group in each drug that can be adsorbed on a metallic surface, resulting in the best DET equilibrium geometries computation and high inhibitory efficiency. The order of inhibitors takes Spiramycin > isosorbide dinitrate.

Acknowledgment

The authors would like to thank the head and members of Department of Applied Sciences, University of Technology- Iraq for their support of the present work.

Conflict of Interests

There are no conflicts of interest regarding the publication of this manuscript.

References

- [1] A. Khammas ,T. Tarish , A. Raidha, A. Khudair,"Evaluation of Hot Corrosion Properties for Nano-coated Superalloy", *Journal of Applied Sciences and Nanotechnology*, 2021, vol. 1, no. 1, pp. 7-14,2021. doi:[10.53293/jasn.2021.11208](https://doi.org/10.53293/jasn.2021.11208).
- [2] E. A. Yaqa, R. A. Anaee, and M. H. Abdulmajeed, "Comparative Study of Different Organic Molecules as an Anti-Corrosion for Mild Steel in Kerosene," *Eng. Technol. J.*, vol. 38, no. 3A, pp. 423–430, 2020.

- [3] A.S. Jawad, Q.N. Obaid, S. Al-Musawi, "Cytotoxicity Effect and Antibacterial Activity of Al₂O₃ Nanoparticles Activity against Streptococcus Pyogenes and Proteus Vulgaris", *Journal of Applied Sciences and Nanotechnology*, 2021, Vol. 1, no. 3, pp. 42-50, 2021. doi: [10.53293/jasn.2021.3944.1061](https://doi.org/10.53293/jasn.2021.3944.1061).
- [4] J. Ishwara Bhat and V. D. P. Alva, "A study of aluminum corrosion inhibition in acid medium by an antiemetic drug," *Trans. Indian Inst. Met.*, vol. 64, no. 4-5, pp. 377-384, 2011, doi: 10.1007/s12666-011-0102-9.
- [5] M. Abdallah, I. Zaafarany, S. O. Al-Karane, and A. A. Abd El-Fattah, "Antihypertensive drugs as an inhibitors for corrosion of aluminum and aluminum silicon alloys in aqueous solutions," *Arab. J. Chem.*, vol. 5, no. 2, pp. 225-234, 2012, doi: 10.1016/j.arabjc.2010.08.017.
- [6] H. Kareem, B. J. Hasson, "Developing Strategy for a Successful Antioxidant, Anticancer Activity via an Improved Method Prepared to Porous Silicon Nanoparticles," *Journal of Applied Sciences and Nanotechnology*, vol. 1, no. 4, pp. 1-11, 2021, doi: 10.53293/jasn.2021.3890.1054.
- [7] Z. Yavari, M. Darijani, and M. Dehdab, "Comparative Theoretical and Experimental Studies on Corrosion Inhibition of Aluminum in Acidic Media by the Antibiotics Drugs," *Iran. J. Sci. Technol. Trans. A Sci.*, vol. 42, no. 4, pp. 1957-1967, 2018, doi: 10.1007/s40995-017-0358-y.
- [8] N. Y. S. Diki, G. K. Gbassi, A. Ouedraogo, M. Berte, and A. Trokourey, "Aluminum corrosion inhibition by cefixime drug: experimental and DFT studies," *J. Electrochem. Sci. Eng.*, no. July, 2018, doi: 10.5599/jese.549.
- [9] N. Raghavendra, "Application of Expired Alprazolam Drug as Corrosion Inhibitor for Aluminum in 3 M HCl Environment," *Journal of Science, Engineering and Technology*, vol. 42, pp. 35-42, 2018.
- [10] M. M. Fares, A. K. Maayta, and J. A. Al-Mustafa, "Synergistic corrosion inhibition of aluminum by polyethylene -BN glycol and ciprofloxacin in acidic media," *J. Adhes. Sci. Technol.*, vol. 27, no. 23, pp. 2495-2506, 2013, doi: 10.1080/01694243.2013.787584.
- [11] M. Abdallah and B. A. Al Jahdaly, "Gentamicin, kanamycin and amikacin drugs as non-toxic inhibitors for corrosion of aluminum in 1.0M hydrochloric acid," *Int. J. Electrochem. Sci.*, vol. 10, no. 12, pp. 9808-9823, 2015.
- [12] R. S. Abdel Hameed, E. A. Ismail, A. H. Abu-Nawwas, and H. I. Al-Shafey, "Expired Voltaren drugs as corrosion inhibitor for aluminum in hydrochloric acid," *Int. J. Electrochem. Sci.*, vol. 10, no. 3, pp. 2098-2109, 2015.
- [13] P. O. Ameh and U. M. Sani, "Cefuroxime axetil: A commercially available drug as corrosion inhibitor for aluminum in hydrochloric acid solution," *Port. Electrochim. Acta*, vol. 34, no. 2, pp. 131-141, 2016, doi: 10.4152/pea.201602131.
- [14] C. U. Ibeji, D. C. Akintayo, and I. A. Adejoro, "The Efficiency of Chloroquine as Corrosion Inhibitor for Aluminium in 1M HCl Solution : Experimental and DFT Study," *Jordan J. Chem.*, vol. 11, no. 1, pp. 38-49, 2016, doi: 10.12816/0026487.
- [15] M. M. Motawea, H. S. Gadow, and A. S. Fouda, "Expired Cidamex Drug as Corrosion Inhibitor for," *Global Journal of Researches in Engineering: C Chemical Engineering*, vol. 16, no. 1, 2016.
- [16] R. H. B. Beda, P. M. Niamien, E. B. Avo Bilé, and A. Trokourey, "Inhibition of Aluminium Corrosion in 1.0 M HCl by Caffeine: Experimental and DFT Studies," *Adv. Chem.*, vol. 2017, pp. 1-10, 2017, doi: 10.1155/2017/6975248.
- [17] A. J. Haider, R. A. AL-Rsool, and M. J. Haider, "Morphological and Structural Properties of Cathode Compound Material for Lithium-Ion Battery," *Plasmonics*, vol. 13, no. 5, pp. 1649-1657, 2018, doi: 10.1007/s11468-017-0674-2.
- [18] A. Haider and Z. N. Jameel, "Synthesis and Characterization of TiO₂ Nanoparticles via Sol- Gel Method by Pulse Laser Ablation" *Eng. & Tech. Journal*, vol. 33, no. December 2016, pp. 3-4, 2015.

- [19] S. H. Salim, R. H. Al-Anbari, and A. J. Haider, "Polymeric Membrane with Nanomaterial's for Water Purification: A Review," *IOP Conf. Ser. Earth Environ. Sci.*, vol. 779, no. 1, 2021, doi: 10.1088/1755-1315/779/1/012103.
- [20] A. J. Haider, "Formulation of Curcumin in Folate Functionalized Polymeric Coated Fe₃O₄ @ Au Core-Shell Nanosystem for Targeting Breast Cancer Therapy," pp. 1–18, 2022.
- [21] A. J. Haider, A. A. Jabbar, and G. A. Ali, "A review of Pure and Doped ZnO Nanostructure Production and its Optical Properties Using Pulsed Laser Deposition Technique," *J. Phys. Conf. Ser.*, vol. 1795, no. 1, 2021, doi: 10.1088/1742-6596/1795/1/012015.
- [22] N. Raghavendra, "Antifebrin Drug Prepared via One-Stage Green Method as Sustainable Corrosion Inhibitor for Al in 3 M HCl Medium: Insight from Electrochemical, Gasometric, and Quantum Chemical Studies," *Surf. Eng. Appl. Electrochem.*, vol. 56, no. 2, pp. 235–241, 2020, doi: 10.3103/S106837552002012X.
- [23] S. Bashir, H. Lgaz, I. M. Chung, and A. Kumar, "Effective green corrosion inhibition of aluminium using analgin in acidic medium: an experimental and theoretical study," *Chem. Eng. Commun.*, vol. 0, no. 0, pp. 1–10, 2020, doi: 10.1080/00986445.2020.1752680.
- [24] N. Raghavendra, "Expired naproxen drug as a robust corrosion inhibitor of Al in 3 M hydrochloric acid system," *Songklanakar J. Sci. Technol.*, vol. 42, no. 4, pp. 917–922, 2020.
- [25] M. Abdallah *et al.*, "Sildenafil drug as a safe anticorrosion for 6063 aluminum alloy in acidic and alkaline solutions: Theoretical and experimental studies," *Egypt. J. Pet.*, vol. 29, no. 3, pp. 211–218, 2020, doi: 10.1016/j.ejpe.2020.06.001.
- [26] I. G. Akande, O. S. I. Fayomi, and O. O. Oluwole, "Anticorrosion Potential of Inhibitive Suphtrim Drug on Aluminium Alloys in 0.5 M H₂SO₄," *J. Bio- Tribo-Corrosion*, vol. 6, no. 4, pp. 1–8, 2020, doi: 10.1007/s40735-020-00429-9.
- [27] R. A. Anaee, "Behavior of Ti/HA in Saliva at Different Temperatures as Restorative Materials," *J. Bio-Tribo-Corrosion*, vol. 2, no. 2, pp. 1–9, 2016, doi: 10.1007/s40735-016-0036-1.
- [28] T. A. Alkarim, K. F. Al Azawi, R. A. Anaee, "Anticorrosive properties of Spiramycin for aluminum in acidic medium", *Int. J. Corros. Scale Inhib.*, vol.10, no. 3, pp.1168–1188,2021.
- [29] R. A. Anaee, M. H. Abd Al-Majeed, S. A. Naser, M. M. Kathem, and O. A. Ahmed, "Antibacterial inhibitor as an expired metoclopramide in 0.5 M phosphoric acid," *Al-Khwarizmi Eng. J.*, vol. 15, no. 1, pp. 71–81, 2019.
- [30] J. George, J. C. Prasana, S. Muthu, and T. K. Kuruvilla, "Spectroscopic (FT-IR , FT Raman) and Quantum Mechanical Study on Isosorbide Mononitrate by Density Functional Theory .," *Int. J. Mater. Sci.*, vol. 12, no. 2, pp. 302–320, 2017.
- [31] K. F. Al-Azawi, I. M., S.Al-Baghdadi *et al.* " Experimental and quantum chemical simulations on the corrosion inhibition of mild steel by 3-((5- (3,5 dinitrophenyl)-1,3,4thiadiazol-2yl)imino)indolin-2-one.," *Results Phys*, vol.9, pp.278–83,2018.
- [32] R. A. Anaee, I. H. R. Tomi, M. H. Abdulmajeed, S. A. Naser, and M. M. Kathem, "Expired Etoricoxib as a corrosion inhibitor for steel in acidic solution," *J. Mol. Liq.*, vol. 279, pp. 594–602, 2019, doi: 10.1016/j.molliq.2019.01.169.
- [33] E. A. Yaqo, R. A. Anaee, M. H. Abdulmajeed, I. H. R. Tomi, and M. M. Kadhim, "Aminotriazole Derivative as Anti-Corrosion Material for Iraqi Kerosene Tanks: Electrochemical, Computational and the Surface Study," *Chemistry Select*, vol. 4, no. 34, pp. 9883–9892, 2019, doi: 10.1002/slct.201902398.
- [34] A. Salman, K. Al-Azawi, M. Iman, " Experimental studies on inhibition of mild steel corrosion by novel synthesized inhibitor complemented with quantum chemical calculations, *Results Phys*, vol.10, pp.291–6,2018.

- [35] F. M., Abdul- Hameed.; Ph.D. thesis. synthesis and characterization of some new mannich bases complexes derived from bis ring oxadiazole of possible biological activity s.; Uⁿ-bnniversity of Baghdad college of science for women; Iraq; 2007.
- [36] S. A., Al- Janabi, M. Kadhim, A. I. Al-Nassiry and T. Yousef "Antimicrobial, computational, and molecular docking studies of Zn (II) and Pd (II) complexes derived from piperidine dithiocarbamate." *Applied Organometallic Chemistry*, 35 (2), pp:6079, 2021.
- [37] A. H. Radhi, A.B. Enass, F. A. Khazaal, Z.M. Abbas, O.H. Aljelawi,"HOMO-LUMO Energies and Geometrical Structures Effecton Corrosion Inhibition for Organic Compounds Predict by DFT and PM3 Methods'. *NeuroQuantology*, pp:37-45,2021.
- [38] F. A. Khazaal, M.M. Kadhim, H.F. Hussein, et al. "Electronic Transfers and (NLO) Properties Predicted by AB Initio Methods with Prove Experimentally'",*NeuroQuantology* 18(1), pp:46-52,2020.
- [39] T. Koopmans, 'Über die zuordnung von wellen funktionen und eigenwerten zu den einzelnen elektronen eines toms'. *Physica.*, 1, pp: 104-113,1933.
- [40] A. Rauk., "Orbital Interaction Theory of Organic Chemistry".2^{ed} Edition. John Wiley & Sons: NewYork, pp.40,2021.
- [41] R. M. Kubba., M.M.Khathem., " Theoretical studies of corrosion inhibition efficiency of two new N-phenyl-ethylidene-5- Bromo isatin derivatives". *Iraqi Journal of Science*, pp.1041-1051, 2016.
- [42] E. A.Yaqo., R. A. Majid., M.H.Abdulmajeed and M. M. Khadim., " Electrochemical, morphological and theoretical studies of an oxadiazole derivative as an anti-corrosive agent for kerosene reservoirs in Iraqi refineries", *Chemical Papers*,vol. 4,pp.98, 2019.
- [43] M. M. Kadhim, R.M. Kubba, "Theoretical Investigation on Reaction Pathway, Biological Activity, Toxicity and NLO Properties of Diclofenac Drug and Its Ionic Carriers, "*Iraqi Journal of Science*, Vol. 61, No. 5, pp. 936-951, 2020.